Generation of 3D Canonical Anatomical Models:
An Experience on Carpal Bones

Imon Banerjee[1], Hamid Laga[2], Giuseppe Patanè[1], Sebastian Kurtek[3], Anuj Srivastava[4], and Michela Spagnuolo[1]

[1] CNR-IMATI, Genova, Italy,
{imon.banerjee, giuseppe.patane, michela.spagnuolo}@ge.imati.cnr.it,
[2] University of South Australia,
Hamid.Laga@unisa.edu.au
[3] The Ohio State University,
kurtek.1@stat.osu.edu
[4] Florida State University,
anuj@stat.fsu.edu

Abstract. The paper discusses the initial results obtained for the generation of canonical 3D models of anatomical parts, built on real patient data. 3D canonical models of anatomy are key elements in a computer-assisted diagnosis; for instance, they can support pathology detection, semantic annotation of patient-specific 3D reconstructions, quantification of pathological markers. Our approach is focused on carpal bones and on the elastic analysis of 3D reconstructions of these bones, which are segmented from MRI scans, represented as 0-genus triangle meshes, and parameterized on the sphere. The original method [8] relies on a set of sparse correspondences, defined as matching vertices. For medical applications, it is desirable to constrain the mean shape generation to set-up the correspondences among a larger set of anatomical landmarks, including vertices, lines, and areas. Preliminary results are discussed and future development directions are sketched.

Keywords: Medical data, carpal bones, Shape analysis, mean shape.

1 Introduction

Thanks to the widespread availability of medical imaging devices, digital 3D data of patients are more and more used, accurate and massive. Diagnosis, image-guided surgery, prosthesis fitting or legal medicine now heavily rely on the analysis of 3D information, such as data measuring the spatial extent of organs, tissues, cells, and even molecules. While there is an agreement on the importance of patient-specific models of the human body, there is still a huge gap between patient data and actual 3D models able to simulate digitally the specificity of each patient, the complexity of the human body, and its anatomical sub-systems (e.g., cardiovascular, musculoskeletal, gastrointestinal systems).

The shape of anatomical structures is highly important: shape is, indeed, related to function and its deviation from a *normality* might indicate pathological

situations. The shape variability, even within healthy situations, is considerable: statistical shape models have been used for guiding 3D image segmentation [11] and cope with the variability of shapes in this phase of medical data analysis. This fact made it difficult until now to exploit fully the usage of 3D reconstructions of anatomical parts for supporting diagnosis or follow-up studies.

In this paper, we explore the suitability of statistical shape analysis to produce 3D *canonical models* of bones, built from homogeneous classes of 3D bone reconstructions, extracted from MRI data. Starting with the method proposed in [8], our aim is to generate a 3D model that captures the variability exhibited by the members of the class, while preserving important anatomical landmarks, which characterize both the function and status of the anatomical part. We argue that 3D canonical models could be used to support diagnosis of musculoskeletal diseases, acting as reference 3D atlases (healthy average shape) based on which important morphometric parameters can be evaluated and quantified.

The paper is organized as follows. First (Sect. 2), we describe the role of 3D canonical models in medicine and give more details on the type and number of anatomical landmarks that are relevant for describing carpal bones. Then (Sect. 3), we introduce the reference framework for the generation of mean shapes, which uses the definition of a shape space constructed from a sparse set of corresponding shape landmarks. The two approaches to 3D mean shape generation, augmented by anatomical landmarks, are described together with the experimental setting. Finally (Sect. 4), our preliminary results are discussed and future work is presented (Sect. 5).

2   3D canonical models in the medical domain

There is an agreement in medicine that both spatial data (e.g., drawings, 2D/3D image, 3D models) and symbolic information (e.g., texts, taxonomies, bio-medical ontologies) have equal importance for describing the human anatomy, and the optimal solution goes in the direction of a tighter integration of the two [2]. Moreover, a comprehensive integration between patient-specific geometric data and symbolic information is required to bring 3D patient-specific models (3D-PSM) fully into clinical practice: this challenging research direction mainly builds on the processes required to (i) extract automatically 3D models from acquisitions (e.g., MRI, CT) and to (ii) characterize the 3D reconstructions according to the needs of the bio-medical domain.

The paper addresses the bridge between (i) and (ii), investigating an approach to define canonical 3D models of anatomy, which encapsulates and integrates medical knowledge (e.g., presence of anatomical landmarks) and shape variability (i.e., statistical variations within an anatomical class). This idea will be discussed focusing on statistical 3D atlases of carpal bones. The wrist joint consists of eight carpal bones-hamate, scaphoid, trapezium, trapezoid, pisiform, triquetrum, capitate. In general, each carpal bone has complex and variable geometry, and knowledge about healthy shape variations is essential for the diagnosis of wrist pathologies, such as osteoarthritis or rheumatoid arthritis.

Today, various digital 3D atlases [3, 10] are available and the access to spatial digital entities tagged with appropriate symbolic information provides an optimal understanding of generic anatomical knowledge. This kind of 3D atlases are used mostly for educational purposes, while computer-assisted diagnosis systems need more specific and statistically-relevant 3D reference shapes to evaluate the regularity of anatomical structures. We target the definition of patient-derived atlases, and we envisage the definition of methods that, using these atlases, might derive automatically morphometric or morphological values for the relevant parameters and descriptors that are considered crucial for the description of the anatomy and its function.

3D reference models of healthy bones are indeed necessary to automatize a number of operations that could help clinicians in their daily practice: these include, for instance, the comparison of a patient-specific 3D reconstructions with the reference healthy models in order to detect anomalies (e.g., fractures, deformations), monitor changes (e.g., pathology evolution), quantify morphometric parameters (e.g., volume, distal area), or compute markers of pathologies (e.g., scores of bone erosion). Anatomical landmarks are defined as any anatomical feature (e.g., fold, prominence, duct, vessel) consistently presents in a tissue (e.g., bone, muscle) that serves to indicate a specific structure or position, and that helps to determine homologous parts of an organism. For carpal bones, anatomical landmarks can be, for instance, contact area, pressure points, or ligament insertion sites that are located on the boundary of the 3D model. Often, these landmarks can be correlated with geometric features, such as grooves or ridges. An interesting study of the capability of geometric reasoning for the extraction of anatomical landmarks of femur is given in [12]. To treat complex injuries or fractures, or in the diagnosis of musculoskeletal pathologies, such as osteoarthritis or rheumatoid arthritis, clinicians need to have a clear idea about the 3D shape of the patient bones, as well as specific positions and characteristics of these landmarks in the patient.

In the present study, we build a taxonomy of landmarks for carpal bones in OWL language, which formalizes a set of landmarks and has been collected by osteological surveys and clinical literatures, and discussed among medical professionals. The landmarks refer to: (i) *areal features*, which are typically used to describe the shape of the bone, and indicate the correlation of the shape with its function within the articulation (e.g., the articular and non-articular facets of the bone, or prominent features, such as the scaphoid tubercle); (ii) *linear features*, which usually delineate the boundaries between the landmark regions; (iii) *point features*, which typically represent either an extremal feature of the bone, such the tip of a protruded facet, or functional sites within the bone, such as ligament insertion sites. It is important to underline that the landmarks have a varying topological dimension and influence the statistical generation of mean shapes. Given the nature of the landmarks, it is clear that their geometric definition is intrinsically vague and their location, or boundaries, is hardly captured by mathematical formulation. Statistical analysis is therefore much more appropriate to locate them.

3 Statistical shape analysis

The main steps of the statistical analysis are: elastic registration, landmark-guided refinement of the registration, and statistic analysis.

Elastic registration According to [8], we represent anatomical shapes as spherically-parameterized surfaces $f : \mathbb{S}^2 \to \mathbb{R}^3$. Let the set of all such surfaces be $\mathcal{F} = \{f : \mathbb{S}^2 \mapsto \mathbb{R}^3 | \int_{\mathbb{S}^2} |f(\mathbf{s})|^2 d\mathbf{s} < \infty$ and f is smooth$\}$, where $\mathbf{s} = (\theta, \phi)$ are the standard spherical coordinates, $d\mathbf{s} = \sin(\theta)d\theta d\phi$ the standard Lebesgue measure on $\mathbb{S}^2$, and $|\cdot|$ denotes the standard 2-norm in $\mathbb{R}^3$. Let also Γ be the set of all diffeomorphisms of $\mathbb{S}^2$ to itself. With a slight abuse of notation, we assume that all the surfaces in $\mathcal{F}$ have been normalized for translation and scale. Let each surface of interest be manually annotated by n anatomical landmarks and $\mathbf{s}_1, \mathbf{s}_2, \ldots, \mathbf{s}_n$ are their location on $\mathbb{S}^2$, such that $f(\mathbf{s}_i)$, $i = 1, 2, \ldots, n$, become the given landmarks on a parametrized surface f.

With this representation, the elastic registration of two surfaces f_1 and f_2 can be formulated as the problem of finding the optimal rotation $O \in SO(3)$ and diffeomorphism, or re-parameterization, $\gamma \in \Gamma$, such that the distance between f_1 and $(Of_2, \gamma) = Of_2 \circ \gamma$ is minimized:

$$(O^*, \gamma^*) = \arg \min_{SO(3) \times \Gamma} d(f_1, (Of_2, \gamma)), \qquad (1)$$

where $d(\cdot, \cdot)$ is a certain measure of distances between surfaces in $\mathcal{F}$. Kurtek *et al.* [6, 7] showed that the Euclidean distance (or $\mathbb{L}^2$ metric) is not suitable for comparing surfaces in $\mathcal{F}$, and thus for solving the registration problem. In fact, the $\mathbb{L}^2$ metric can lead to non-symmetric registration between f_1 and f_2, and more importantly, the re-parameterization group does not act by isometry under this metric, i.e. $\|f_1 \circ \gamma - f_2 \circ \gamma\| \neq \|f_1 - f_2\|$ unless γ is area preserving, which is often not the case, particularly when dealing with elastic deformations.

To overcome these limitations of the $\mathbb{L}^2$ metric, Jermyn *et al.* [5] proposed a simplified elastic metric that quantifies differences between two surfaces f_1 and f_2 as a weighted sum of the amount of bending and stretching that is needed to align one surface onto the other. Furthermore, they showed that by carefully choosing the weights of the two terms, the metric reduces to an Euclidean distance between the *Square Root Normal Fields* (SRNF) representations of the two surfaces. Formally, the SRNF representation of a surface f is a function $q : \mathbb{S}^2 \to \mathbb{R}^3$ defined as $q(\mathbf{s}) = \frac{n(\mathbf{s})}{\sqrt{a(\mathbf{s})}}$, where $n(\mathbf{s}) = \frac{\partial f}{\partial \theta} \times \frac{\partial f}{\partial \phi}$ is the normal to f at $\mathbf{s} = (\theta, \phi)$ and $a(\mathbf{s}) = |\mathbf{n}(\mathbf{s})|$ is the local surface area at s.

With this representation, the elastic registration problem defined in Eq. (1) can be formulated using the Euclidean metric in the space of SRNFs:

$$(O^*, \gamma^*) = \arg \min_{SO(3) \times \Gamma} \|q_1 - (Oq_2, \gamma)\|^2, \qquad (2)$$

where q_i is the SRNF representation of f_i and $(q, \gamma) = \sqrt{J_\gamma} q \circ \gamma$. Here, J_γ is the determinant of the Jacobian of γ. Note that the Euclidean distance in the space

of SRNFs corresponds to the geodesic distance in $\mathcal{F}$. We refer the reader to [5] and [7] for the theoretical details of this representation and also for the approach used for solving the optimization of Eq. (2). Then, we rotate f_2 with O^* and re-parameterize it with γ^* to obtain a new surface $\tilde{f}_2$ that is in full correspondence with f_1.

Landmark-guided refinement of the registration While the proposed approach finds plausible elastic registrations between surfaces, in many cases, however, it fails to correctly align the anatomical landmarks (provided by medical experts), particularly when the landmarks are located in feature-less regions. We propose to refine the registration by finding an additional diffeomorphism γ_0 that aligns the landmarks of the two surfaces. Let us assume that the surface f_1 is annotated by a number, n, of anatomical landmarks. Let $\mathbf{s}_1, \mathbf{s}_2, \ldots, \mathbf{s}_n$ be the locations of these landmarks on $\mathbb{S}^2$. Similarly, let $\tilde{\mathbf{s}}_1, \tilde{\mathbf{s}}_2, \ldots, \tilde{\mathbf{s}}_n$ be the locations on $\mathbb{S}^2$ of the landmarks of $\tilde{f}_2$. Let us assume that the corresponding landmark pairs are $\{f_1(\mathbf{s}_i), \tilde{f}_2(\tilde{\mathbf{s}}_i)\}$. Following [8], we connect each pair of matched landmarks on $\mathbb{S}^2$ with a great circle and sample it uniformly using k steps ($k = 5$, in our implementation). Then, we solve, using [4], for a small deformation that matches the $(k-1)$-st point to the k-th point on this circle for all j. A composition of these k small deformations leads to the larger desired deformation γ_0. Finally, the composition $\gamma^* \circ \gamma_0$ leads to the optimal diffeomorphism that puts f_2 in full correspondence with f_1.

Summary statistics Let $F = \{f_1, \ldots, f_N\}$ be a set of N spherically-parameterized carpal bone surfaces of the same type. Let also q_i be the SRNF representation of f_i. We seek to build an atlas that is composed of the average shape μ and its modes of variation. The first step is to register all the surfaces into the same coordinate frame. To this end, we first compute the pairwise distances between every pair of surfaces f_i and f_j in F using the geodesic distance defined in Eq. (2). We then select among all the surfaces in F the one that has the minimum average distance to all the other surfaces. Let us denote it by g and note that g corresponds to the medoid point of the set F.

Next, for every surface $f_i \in F$, we find the optimal rotation O_i^* and diffeomorphism γ_i^* that align f_i onto g. Let $\tilde{f}_i = (Q^* f_i, \gamma_i^*)$. Then, all the surfaces $\tilde{f}_i$ are now fully aligned and one can use standard linear statistics to compute the mean shape and the modes of variation. That is, the mean shape μ is given as: $\mu = \frac{1}{N} \sum_{i=1}^{N} \tilde{f}_i$.

Finally, the principal modes of variations can be obtained using standard Principal Component Analysis on the surfaces $\tilde{f}_i$ after discretization. Note that it is possible to compute the summary statistics directly on the non-linear manifold $\mathcal{F}$ by computing for example the Karcher mean [8] and studying the modes of variation on the tangent space to $\mathcal{F}$ at the Karcher mean. This approach, however, can be computationally expensive, particularly when dealing with high resolution data sets.
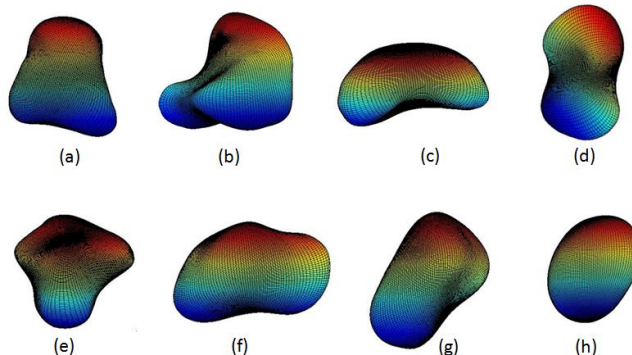
Fig. 1. Mean shape of the bone of the right wrist: (a) capitate, (b) hamate, (c) lunate, (d) scaphoid, (e) trapezium, (f) trapezoid, (g) triquetrum, (h) pisiform.

4 Experiments and discussion

In this case study, we mainly focus on (i) testing the original elastic 3D shape analysis framework with the carpal bone data set, and assessing the quality of resulting 3D mean shapes and (ii) discussing the hypothesis that guarantees that actual anatomical features can be preserved in the mean shape, by using the anatomical landmark-guided correspondence in the mean shape generation step.

Creation of 3D carpal bone data set We have generated and classified a data set that contains two sets of patient-specific carpal bones. The first set contains 49 healthy and pathological subjects segmented from T1 weighted MRI images. On average, for each class of the carpal bone, we have 14 3D surface models for left wrist and 18 surface models for right wrist. Moreover, the data set contains 8 pathological subjects for left wrist and 6 for right wrist. We have augmented this set with the models provided by the Digital database of wrist bone anatomy [9], which contains 30 triangulated 3D models for each carpal bone (healthy) segmented by experts from high-resolution CT images. We manually annotated the 3D models in our training data set [1], using the carpal bone landmark taxonomy, where we have formalized the landmarks mentioned in Sect. 2. Each bone model was annotated with 6-8 landmark regions, where the regions mostly represented the prominent bone features (e.g., hook of the hamate) and articulation facets.

Atlas generation without and with anatomical landmark guided correspondence In Fig. 1, we show a set of mean shapes computed from the carpal bone training data set (healthy subjects) without anatomical landmark guided correspondence. The generated mean shapes loses some anatomical features with respect to the training data set. According to our preliminary results, we derive the hypothesis that the actual anatomical features can be preserved in the mean shape genera-
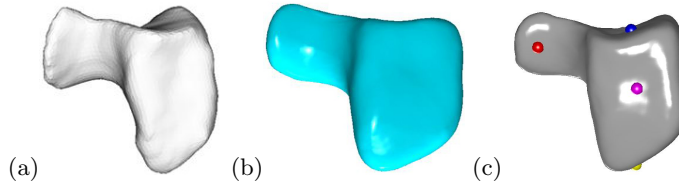
Fig. 2. (a) Input shape (hamate), generated mean shape (b) without and (c) with anatomical landmark guided correspondence.

tion process by applying anatomical landmark-guided refinement of the registration. To verify our hypothesis, we performed experiment by generating the mean shape of the healthy hamate bone (right) based on anatomical landmark-guided correspondences. The anatomical landmarks were manually annotated by the experts on the training data set (16 -18 shapes) using the *SemAnatomy3D* [1] tool, which allows interactive annotation of anatomical landmarks on the 3D models. As the shape generation works with vertex correspondences only, we have established the correspondences between healthy bone models considering only the centroid of each annotated region; e.g., the centroid of the hook of hamate region. In Fig. 2, the anatomical features in the mean shape generated with landmark-guided correspondences (c) appear more reliable and similar to the input shape than the ones generated without taking into account the anatomical landmarks (b). Moreover, another advantage is that the generated mean shape contains the canonical landmark positions, which can be further utilize in several applications (Sect 2).

5   Conclusions and future work

In this paper, we presented a framework that generates canonical 3D models from the real patient data by using an elastic shape analysis guided by the correspondence of anatomical landmarks. The generated models capture the healthy variability while preserving important anatomical landmarks. It can be used as an average healthy shape for supporting the comparison with patient data to detect anomalies or compute markers of pathologies. We introduced the framework with carpal bone case study, but it can be extended to generate canonical model of other anatomical districts. The results presented are preliminary and several steps are necessary to better evaluate the performance of the method. There is an obvious need for a deeper analysis of the results and a validation framework involving experts. On the technical side, we would like to address shape correspondences defined by fully real landmarks. This step requires to design also a more elaborate parametrization method to properly map these constraints during the parametrization step and then use them to guide the correspondences. Once the method is refined, we are also planning to use the 3D canonical model to automatically identify landmarks and transfer the annotation from the template to the patient-specific reconstructions.

References

1. Banerjee, I., Agibetov, A., Catalano, C., Patané, G., Spagnuolo, M.: Semantic annotation of patient-specific 3D anatomical models. In: IEEE Proceedings of the International Conference on Cyberworlds (In press 2015)
2. Banerjee, I., Catalano, C.E., Robbiano, F., Spagnuolo, M.: Accessing and representing knowledge in the medical field: Visual and lexical modalities. 3D Multiscale Physiological Human. Springer London pp. 297–316 (2014)
3. Blume, A., Chun, W., Kogan, D., Kokkevis, V., Weber, N., Petterson, R.W., Zeiger, R.: Google body: 3D human anatomy in the browser. In: ACM SIGGRAPH 2011 Talks. p. 19. ACM (2011)
4. Glaunès, J., Vaillant, M., Miller, M.: Landmark matching via large deformation diffeomorphisms on the sphere. Journal of mathematical imaging and vision 20(1-2), 179–200 (2004)
5. Jermyn, I.H., Kurtek, S., Klassen, E., Srivastava, A.: Elastic shape matching of parameterized surfaces using square root normal fields. In: ECCV. pp. 804–817 (2012)
6. Kurtek, S., Klassen, E., Ding, Z., Srivastava, A.: A novel Riemannain framework for shape analysis of 3D objects. In: IEEE CVPR. pp. 1625–1632 (2010)
7. Kurtek, S., Klassen, E., Gore, J.C., Ding, Z., Srivastava, A.: Elastic geodesic paths in shape space of parameterized surfaces. IEEE Transactions on Pattern Analysis and Machine Intelligence 34(9), 1717–1730 (2012)
8. Kurtek, S., Srivastava, A., Klassen, E., Laga, H.: Landmark-guided elastic shape analysis of spherically-parameterized surfaces. Comper Graphics Forum 32, 429–438 (2013)
9. Moore, D.C., Crisco, J.J., Trafton, G.T., Leventhal, E.: A digital database of wrist bone anatomy and carpal kinematics. Journal of biomechanics 40(11), 2537–2542 (2007)
10. Qualter, J., Sculli, F., Oliker, A., Napier, Z., Lee, S., Garcia, J., Frenkel, S., Harnik, V., Triola, M.: The biodigital human: a web-based 3D platform for medical visualization and education. Studies in health technology and informatics 173, 359–361 (2011)
11. Rajamani, T.K., Styner, A.M., Talib, H., Zheng, G., Nolte, L.P., Ballester, A.: Statistical deformable bone models for robust 3d surface extrapolation from sparse data. Medical Image Analysis 11(2), 99–109 (2007)
12. Subburaj, K., Ravi, B., Agarwal, M.: Automated identification of anatomical landmarks on 3d bone models reconstructed from ct scan images. Computerized Medical Imaging and Graphics 33(5), 359–368 (2009)